MICROCOMPUTER-BASED CONTROLLER

OF COUPLED FLUID PRESSURES

IN TRIAXIAL STRESS TESTING

by

JERALD PAUL MENOZZI JR.

SUBMITTED TO THE DEPARTMENT OF
ELECTRICAL ENGINEERING AND COMPUTER SCIENCE
IN PARTIAL FULFILLMENT OF THE
REQUIREMENTS FOR THE
DEGREE OF

BACHELOR OF SCIENCE

at the

MASSACHUSETTS INSTITUTE OF TECHNOLOGY

February 1985

Signature of Author Signature Redacted
ering
puter Science
ry 30, 1985

Certified by Signature Redacted

Dr. Robert T. Martin
Thesis Supervisor

Accepted by Signature Redacted

Prof. David Adler
Chairman, Department Committee

MICROCOMPUTER-BASED CONTROLLER
OF COUPLED FLUID PRESSURES
IN TRIAXIAL STRESS TESTING

by

JERALD PAUL MENOZZI JR.

Submitted to the Department of Electrical Engineering
and Computer Science on January 30, 1985
in partial fulfillment of the requirements
for the degree of Bachelor of Science
at the Massachusetts Institute of Technology

Abstract

The Resource Extraction Laboratory at MIT conducts laboratory simulations of both artificially induced and naturally occuring geological phenomena. The materials used to model subsurface rock in these simulations are cement- based composites, for which the material properties must be determined. A computer-based triaxial test cell capable of testing a wide range of material properties is being developed. That cell houses a ram piston, which applies axial stress to specimens during strength testing. A control algorithm for the control of ram piston hydraulic fluid pressure was developed in this thesis.

The fluid power circuit was modelled by a lumped parameter circuit. It contained elements whose constitutive laws relating fluid pressure to fluid flow rate were found to be non-linear–namely valves. An analog computer simulation on which to test non-linear control algorithms was desired, but an electrical analog to the servo-valves in the circuit could not be found.

Tests were run on the vessel itself in which the response of vessel pressure to a step in input pressure was compared to a first order linear system response. Further tests revealed that pressure in the vessel rose quite linearly in the vessel from the opening of the valve out to times on the order of the control program's sampling period. This fact was utilized in the control algorithm described in detail in Chapter 5. The algorithm has not yet been installed in a computer program and tested on the vessel.

Table of Contents

List of Figures

List of Tables

Acknowledgements

Thanks, Professor Cleary, Dr. Martin, Rich, Suki, Steve, Tim, Christine, Barry, Mohan, Geez, I hope I'm not forgetting anyone...John, Marcia, Maria, Dad, Scott, Chris, JEP, Steve the cat... Oh yea, and especially you, Mom.

1.Introduction

The MIT Resource Extraction Laboratory, *REL*, develops theoretical models of geological phenomena. Depending on their accuracy, geological models allow an engineer to make predictions about the response of subsurface formations to certain conditions. In the field of resource extraction, specifically in hydraulic fracturing, these models are of great value. They are also useful in the study of related naturally occuring phenomena, such as pore pressure induced cracking, *PPIC*.

Laboratory simulations test the models developed at *REL*. In order to successfully simulate conditions present in an underground rock formation, both the stress conditions within the rock and its own material properties must be accurately modeled at the surface. As a result, cement-based composites are subjected to highly controlled stress conditions imposed by a triaxial test cell in *REL* simulations.

The remainder of this thesis deals with the development of a computer-based control system for the fluid power system of a 30,000 psi triaxial cell. First, a description of the tests to be performed will be given, along with a discussion of the advantages of a computer-based system over the old system. Next the approach taken in designing the system will be discussed in some detail, including problems encountered and approximations made. Test results and an accompanying discussion will follow. Finally, the project's state of completion will be assessed and recommendations for continued work will be made.

2. Material Properties Testing at REL

2.1 The Significance of Material Properties

The types of models developed and tested at *REL* are highly dependent on, among other things, knowledge of the material properties of the rock involved. For these models to be utilized in field situations, actual samples of rock would be extracted and tested. The accuracy of this testing would greatly affect the success of the model.

Periodic testing of these models takes place in laboratory environment during their development. In order for these tests to produce meaningful results, at least the following two things must be assured. First, the conditions present during the test must closely represent the conditions in the field where the model will be applied. Second, the properties of the material used in the model must be accurately determined. An error in the measurement of properties could be falsely construed as an error in the theoretical model.

Cement-based composites, *CBC*'s, are used as model rock at *REL* for a couple reasons. First, their poroelastic properties closely resemble those of sandstone and other types of rock from which oil is commonly extracted. Second, the *CBC*'s used can be cast with relative ease into samples compatible with the test equipment. Following are two examples of lab simulations and the types of *CBC*'s they use.

In the Crack Interaction Test, the behavior of hydraulically driven cracks at material boundaries is studied. For this test, cement paste blocks cast 10" in diameter by 14" in length are tested in a 2000 psi triaxial cell. The cement paste used is composed of cement and water in a 1.0:0.5 ratio. This experiment is described in detail by Wright [1984]. *PPIC* experiments use cement mortar specimens 4" in diameter and varying in length. Casting and curing of the cement mortar, of composition 1.0:1.0:0.8, sand:cement:water, is described by Vogeler [1984]. The methods of testing these two *CBC*'s, cement paste and cement mortar, including the preparation of test specimens, are described in Section 2.4.

2.2 Material Properties of Interest

Cement-based composites, like other porous materials, can be characterized by a set of poroelastic properties – some are directly measurable, while some are lumped material parameters, involving one or more measurable parameters. A list of properties of porous *CBC*'s tested at *REL* includes permeability, porosity, B factor, diffusivity, Young's modulus, and Poisson's ratio. Properties testing, including experimental procedures and results, is covered by Martin, et al. [1984].

Of particular interest in this thesis are the poroelastic properties involved in stress-strain relationships and material strength. *CBC*'s are regarded as elastic materials, though they may also exhibit the rheological properties of viscosity and plasticity, depending on the state of stress and the rate of straining. The elastic behavior of the *CBC*'s tested in the lab, which are relatively homogeneous and isotropic, can be completely characterized by two constants. They are Young's modulus (E), the ratio of axial strain to axial stress, and Poisson's ratio (ν), the ratio of lateral strain to axial strain. Continuous materials, such as underground rock formations, can be characterized by the following alternative pair of constants. Bulk modulus (K), is the ratio of bulk stress to volumetric strain, while the shear modulus (G), is the ratio of deviatoric stress to deviatoric strain [Hawkes and Mellor, 1969].

2.3 Uniaxial vs. Triaxial Testing of Elastic Properties

Stresses in materials in which no shear stresses exist, can be lumped into 3 components or principle stresses. When referring to a continuous medium, such as an underground rock formation, the stress state at a point is resolved into 1 vertical and 2 horizontal components. In the case of a discrete element, such as a test specimen, principle stresses, shown in Figure 1, are named according to their relative magnitude and direction. The component representing the greatest compressive stress is usually considered the major principle stress (σ_1). The other two are referred to as intermediate (σ_2) and minor (σ_3) principle stresses.

In stress-strain testing, principle stresses can be specified by the loading apparatus. The distinction between uniaxial and triaxial stress testing is made based on which stresses can be independently controlled during the test. Ideally, in a uniaxial compressive test, there should be only one finite principle stress throughout the specimen. In triaxial testing, complex stress fields are possible due to independent control over the 3 principle stresses. It is typical, however, for triaxial tests to be run with the intermediate and minor principle stresses equal. One example of a typical test is the cylindrical comperession test, which is the type of test run at *REL*. σ_2 and σ_3 are equal and are applied to the sample via a confining fluid. σ_1 is then applied by a ram piston. Deviator stress, ($\sigma_1 - \sigma_3$), may be varied throughout the experiment.

One additional characteristic of a triaxial test of porous materials is the drainage conditions imposed on the sample. Porous materials exhibit stress-strain characteristics which are dependent, not only on the properties of the solid skeleton material, but also on the pressure of the fluid in the void space. In undrained materials, in which the fluid pressure or *pore pressure* does not equal zero, the elastic behavior is determined by the effective stress (σ'), which is the difference between total normal stress (σ) and the pore pressure (p) [Bishop and Henkel, 1957].

$$\sigma' = \sigma - p \qquad (1)$$

In order to do meaningful testing on porous materials, drainage conditions must be closely monitored and controlled. A triaxial test system should be able to support tests under all drainage conditions. According to Bishop and Henkel [1957], the following three drainage conditions exist:

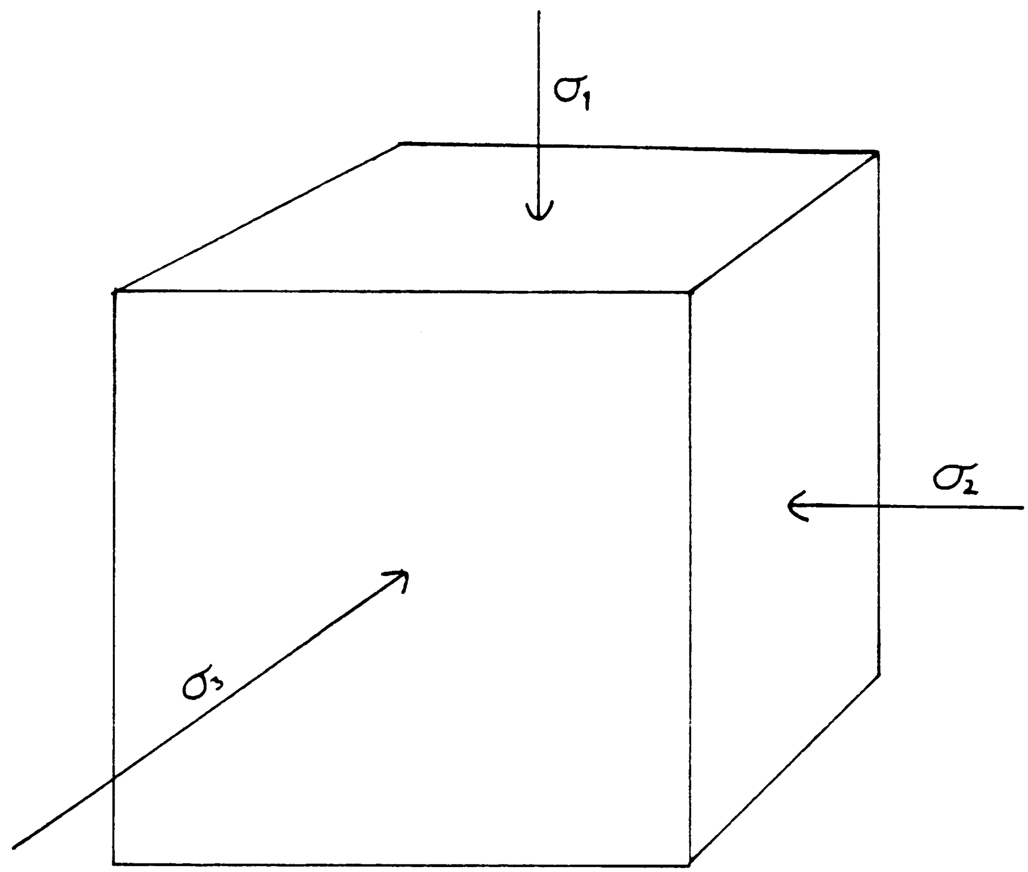

Figure 1. The Principle Stresses on an Element of Material

a) Undrained tests where there is no drainage during the application of uniform triaxial stress so no dissipation of pore pressure occurs. No drainage is allowed during the application of deviator stress.

b) Consolidated-undrained tests, where drainage is allowed during the application of uniform triaxial stress, but no drainage is allowed during the application of deviator stress.

c) Drained tests, where drainage is permitted throughout the test and no excess pore pressure is set up during the application of deviator stress.

The relationship of pore pressure, triaxial strain, and triaxial stress to the elastic properties E, and , is indicated by the following equations. The first three represent changes in effective stresses upon the application of principle stresses. The fourth equation relates volume change of the specimen to the effective stresses and the elastic properties, Young's modulus (E), and Poisson's ratio (ν) [Bishop and Henkel, 1957].

$$\begin{aligned} \Delta\sigma_1' &= \Delta\sigma_1 - \Delta p \\ \Delta\sigma_2' &= \Delta\sigma_2 - \Delta p \\ \Delta\sigma_3' &= \Delta\sigma_3 - \Delta p \end{aligned} \qquad (2)$$

$$-\Delta V = V\frac{(1-2\nu)}{E}\left(\Delta\sigma_1' + \Delta\sigma_2' + \Delta\sigma_3'\right) \qquad (3)$$

In the absence of pore pressure, tests to determine Young's modulus and Poisson's ratio may be conducted uniaxially on unjacketed samples. However, results of these tests can be used only to approximate the elastic properties of undrained material, which is prevalent in underground formations. In order to test for the properties of undrained materials confining stress must be specified and held constant during the application of deviator stress. The rate of deviator stress must also be specified and held constant throughout the test. Axial and radial strain (in the case of cylindrical specimens), as well as pore pressure must be monitored in real time. These test requirements have motivated the use of computer control for the triaxial test system.

2.4 Previous Test System

Samples used in elastic properties testing are 4" in diameter and 8" in length, since it has been found that 2:1, length to diameter, ratio minimizes the end-effects of axial loading on radial and axial strain. Samples in the desired 2:1 ratio were obtained by sawing to length the mortar samples and by both coring and sawing to length the paste samples. Tests were run on samples with curing times ranging from 3 to 40+ days.

Previously, testing of elastic properties was conducted uniaxially by applying an axial stress to an unconfined specimen. Radial extensometers equipped with semiconductor strain guages were placed on the specimen to monitor radial strain, while displacement transducers were used to measure axial strain. A compressive load was applied with a Baldwin Compression machine to specimens fitted with fluid filled end pads. A pressure transducer in an end pad allowed the pressure of the end pad fluid, which is equal to the applied stress, to be monitored. Both strain and applied stress data were monitored by a DEC Minc-11 microcomputer. For a complete description of test equipment, refer to Appendix E of Martin et al., [1984].

In anticipation of a triaxial test system, procedures for determining elastic properties were revised during the summer, 1984, to accomodate testing for both drained (E, ν) and undrained (E_u, ν_u) properties. However, all testing done to date has been uniaxial, using the equipment described above. The unconfined samples were loaded up to 900 psi and then unloaded to 0 psi. Radial and axial strain and axial stress were monitored during loading and unloading, in order to determine E and .

Undrained tests can be run uniaxially (unconfined) if loading and unloading takes place fast enough that no drainage occurs. In the case of drained tests, the loading rate needs to be slower by at least a factor of 10 in order to allow the specimen to drain during the test. Since the drainage of specimens prior to testing was not closely controlled, drained tests were run over a period of 10 minutes in order to avoid the effects of pore pressure.

2.5 New Computer-based Triaxial Test System

Test samples used with the new test system will be prepared similarly to those described in Section 2.4, with one major difference. Since samples in the triaxial cell will be surrounded by a confining fluid, they must be jacketed in order to isolate pore fluid from confining fluid. Several methods of jacketing samples have been attempted. The biggest problem encountered has been leakage, which prohibits the maintenance of separate pore pressure and confining pressure. Success has been achieved with Devcon Flexane 80 Liquid. Several specimens have been jacketed with this epoxy without a leak. Details of the jacketing process can be found in Appendix C of Martin et al., [1984].

The new triaxial system is built around a 30,000 psi pressure vessel. An internal hydraulically-driven ram piston applies axial stress to a sample placed between it and the cover. The internal chamber of the vessel is 24" deep and the ram itself is 12" long. This leaves less than 12" for the sample and end caps since the ram is not allowed to reach the bottom of the chamber. In the space around the sample, a confining stress is applied via pressurized confining fluid. See Figure 2 for a schematic diagram of the cell.

Confining fluid pressure and ram piston hydraulic fluid pressure are controlled by two separate fluid power circuits. The ram pressure circuit derives its power from an air-driven, differential-area piston pump, capable of producing 50,300 psi

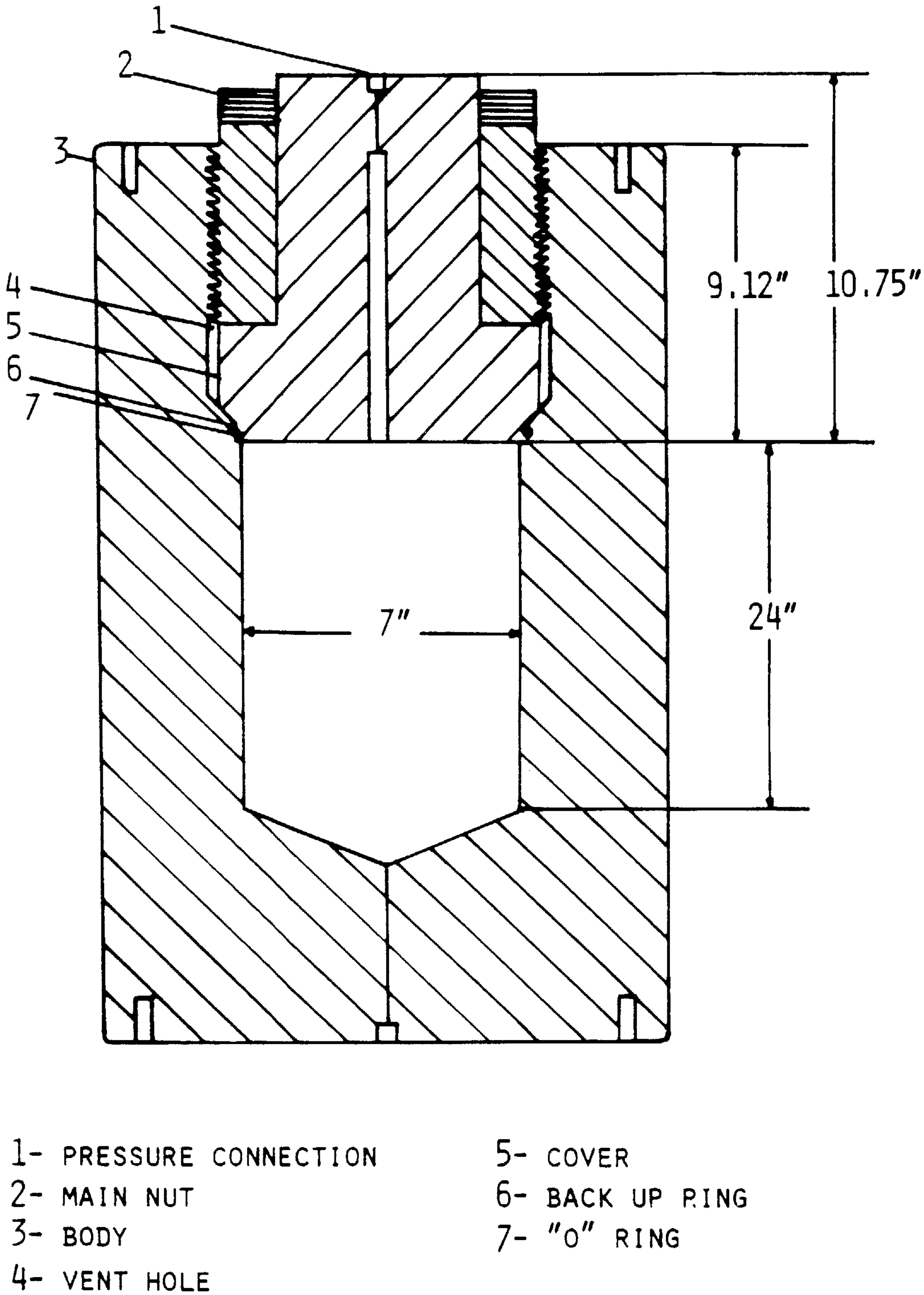

Figure 2. 30,000 PSI Triaxial Test Cell

static, hydraulic pressure when supplied with dry air at 110 psi. Fluid supplied to the pump from a 40 psi reservoir is pumped through 1/8" *ID* high pressure tubing to a high pressure tee. Lines branching off the tee lead to two servo-valve assemblies – one acting as a drain valve, leading back to the reservoir, and the other functioning as a control valve, regulating flow, and therefore pressure, into the vessel. A symbolic representation of the ram fluid power circuit appears in Figure 3. The confining fluid is pressurized by a similar circuit.

An IBM PC microcomputer-based feedback control system, designed to regulate ram pressure, recieves pressure data from a transducer between the control valve and the vessel. Analog to digital conversion of the transducer data is accomplished with a data aquisition and control system. Control is then asserted via digital outputs to the digital control circuitry of the servo-valve. An explanation of the design of the control algorithm appears in Chapters 3 and 5.

The new system was developed for testing specimens across a wide range of pressures (up to 30,000 psi) and over a range of loading rates. It can accurately model the stress conditions of subsurface formations at a wide range of depths. Test results with this system will lead to a more comprehensive data base. The requirements dictated the use of a pressure vessel in which confining stress and axial stress could be controlled independantly. With the proper plumbing in place and the automatic control system functional, tests will be conducted at any pressure within the safe range of the vessel and at any rate within the capabilities of the control system. Stress-strain and pore pressure data will be monitored and recorded as before, as well as displayed on real-time graphs.

A more detailed description of the components of the new system, including manufacturers and model numbers, appears in Appendix A.

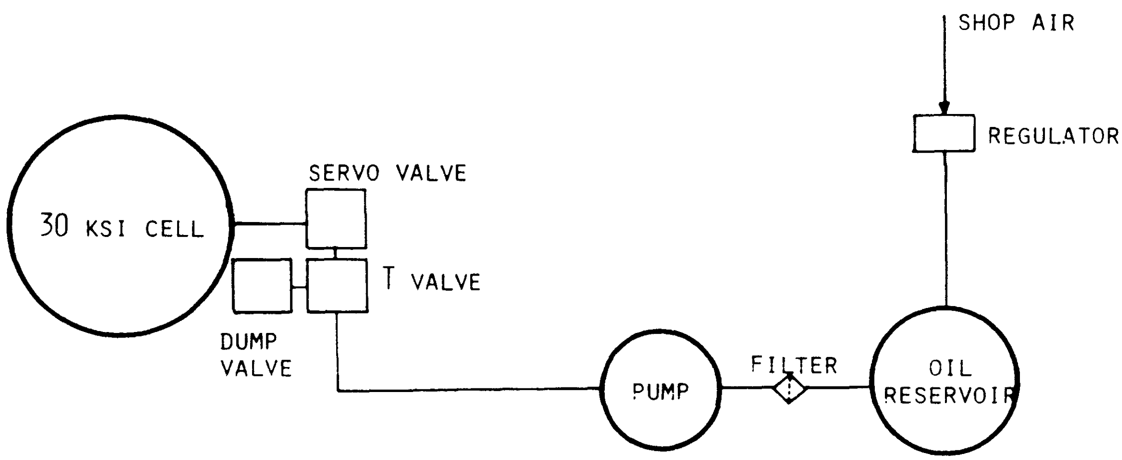

Figure 3. Symbolic Representation of Ram Piston Hydraulic Fluid Power Circuit

3. Design of Triaxial Cell Fluid Pressure Control System

3.1 Approach to Control System Design

Computers have allowed much freedom in the design of control systems for both linear and non-linear systems. In the linear case, both classical and modern control theory lend themselves nicely to computer implementation. Both require merely a knowledge of the linear differential equations describing the system to be controlled. Once this is known, a control system may then be designed to exhibit a desired response. In a classical control solution, the poles of the system may be moved from their open loop positions to anywhere along a set of points called the *root locus*, depending on the amount of gain applied. The placement of the poles will in turn determine the response of the system to a particular excitation. By using compensation, a technique which adds poles and zeros to the system, the root locus may be changed to produce nearly any desired response. Familiar classical control solutions include proportional or *dead beat* controllers, along with proportional, plus derivative, plus integral or *PID* controllers. In modern control, feedback ratios or gains are a function of the open loop poles of the system. A wide range of closed loop responses are possible by specifying the desired poles via feedback ratios.

Non-linear control solutions are not so straightforward. They generally require a creative algorithm and much more computational power than their linear counterparts. However, some non-linear systems may be modeled as linear in a small range around the operating point of the input. Others may be modeled as piecewise-linear, with the constant of proportionality being dependent on the particular range of operation. In either case, linear control algorithms will work, provided the appropriate restrictions are imposed.

The first step in designing a control system is to model the system using lumped parameters to represent actual system elements. Lumped parameter models are easily translated into the mathematical equations with which the control system is designed. At this point, it can be determined whether or not the system is linear and, if it is not, whether or not it can be linearized. This step was taken in designing the present control system and is summarized in the following section.

3.2 Developing a Mathematical Model of the System

A mathematical model not only leads to the system equations from which the control program may be written, but also allows an analog computer simulation to be designed. As long as every element in the actual system has an electrical analog, and the analogous electrical components are connected in the same topology, system response may be studied using the electrical model. This approach is useful in cases where it may be too costly or cumbersome to run tests using the actual system. Or it may be used in the design phase to study the response of the prospective system to particular inputs. Analog computer simulations also provide a convenient proving ground for control program development, especially when the actual system is still under construction.

An analog computer simulation was planned as part of this control program development, since plumbing of the ram fluid power circuit was not yet completed. A lumped parameter model was developed, but turned out to contain non-linear elements which had no electrical counterpart. Consequently, the analog computer simulation was abandoned. The fact that the system was non-linear also precluded the use of linear control techniques. The model was retained, however, for possible use in developing the control system.

The fluid power circuit for the triaxial test cell is drawn schematically in Figure 3. Each element in the system, including the lengths of pipe, was modeled by an idealized element and interconnected in a circuit diagram in Figure 4. To a first approximation, certain effects were ignored in the model. For instance, effects analogous to electrical inductance, called fluid inertance, were left out of the model because,in the case of nearly steady flow, pressure drop due to fluid inertance is nearly zero. This can be seen by the element's constitutive relationship, in which Q is flow rate, $\triangle P$ is pressure drop across the element, and I is the fluid inertance [Shearer, Murphy, and Richardson, 1971].

$$\Delta P = I \frac{dQ}{dt} \quad (4)$$

Fluid inertance results from the inertia of moving a mass of fluid in a length of pipe. It is a lumped parameter dependent on the density of the fluid (ρ), the length of pipe (l), and its cross-sectional area (A) in the following relationship.[Shearer, et al., 1971].

$$I = \frac{\rho l}{A} \quad (5)$$

Its effect takes place at every point between the two ends of the pipe and is known a distributed effect. In a lumped parameter model circuit the inertance must be lumped into a single element connecting two nodes of the circuit. This can cause problems in the case where another effect, for instance a fluid resistance, is acting between the same two nodes. The pressure drops due to both effects obviously sum to give the pressure drop between the two nodes and the two elements should, therefore, be in series in the model circuit. However, this introduces a "phantom" node between the elements which doesn't really exist. This situation illustrates one of the limitations of lumped parameter models.

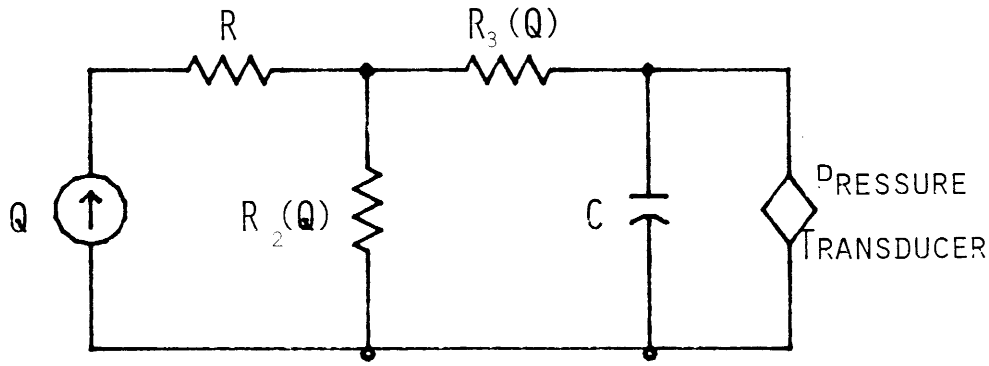

$$Q^2 = \frac{C_V{}^2 \Delta P}{(SG)}$$

$$\frac{\Delta P}{Q} = \frac{Q(SG)}{C_V{}^2} = R(Q)$$

Figure 4. Lumped Parameter Model of Fluid Power Circuit

Fluid resistance in pipes is dependent mainly on the viscosity of the fluid, the dimensions of the pipes, and their Reynolds numbers. Unlike the electrical resistance of interconnecting wires, fluid resistance in pipes is often not negligible. Whether flow is laminar or turbulent depends on the pipe's Reynolds number (Re), which is given by the following equation in which ρ is fluid density, μ is fluid viscosity, Q is flow rate, and d is pipe diameter [Shearer, et al., 1971].

$$Re = \frac{4\rho Q}{\pi d \mu} \tag{6}$$

The regime of laminar flow is generally considered to include Reynolds numbers up to approximately 2300 [White, 1979]. Anything above 5000 is usually considered fully turbulent. For laminar flow only, under certain conditions, the constitutive law for the fluid resistance of a length of pipe is linear. First, inertial effects must be small. Second, the pipe must be long compared to the entrance length, the distance beyond the opening at which turbulent flow ceases and the flow becomes totally laminar. The constitutive relation between pressure drop and laminar flow under these conditions is

$$\Delta P = RI \tag{7}$$

where the fluid resistance (R) is described by the following equation, in which μ, l, and d represent the same quantities as above. [Shearer, et al.,1971].

$$R = \frac{128 \mu l}{\pi d^4} \tag{8}$$

Flow was found to be limited to laminar in all lengths of pipe in the circuit for flow rates up to the maximum required by the system. Values computed for the Reynolds number and entrance length at maximum flow rate, and the fluid resistance of all lengths of pipe in the circuit are shown in Table 1.

The pressure vessel was modeled as a fluid capacitance, an element in which fluid energy storage is due to fluid compliance. The compliance of the vessel was neglected. Fluid inertia and frictional effects in the vessel were also neglected.

Pipe Segment	Reynolds Number	Entrance Length	L_E / L_{TOT}	Resistance
1	10.927	.002m	.39%	$108.2 \frac{Ns}{m^5}$
2	10.927	.002m	2.34%	$17.8 \frac{Ns}{m^5}$
3	3.642	.002m	.13%	$4.0 \frac{Ns}{m^5}$
4	10.927	.002m	2.19%	$19.0 \frac{Ns}{m^5}$
5	10.927	.002m	1.13%	$36.9 \frac{Ns}{m^5}$
6	5.464	.002m	1.06%	$2.5 \frac{Ns}{m^5}$

Table 1. Fluid Resistances of Pipes in Fluid Power Circuit

The value of the vessel's fluid capacitance is given by the following equation, in which V represents the volume of the vessel, and β represents the bulk modulus of the fluid [Shearer, et al., 1971].

$$C = \frac{V}{\beta} \tag{9}$$

Since the apparent volume of the vessel changes as the ram piston moves up, the fluid capacitance is not really linear, and can be found to be a function of pressure. However, movement of the ram causes only a 2.3% volume change, which was considered negligible. The constitutive law relating pressure and flow into the vessel is shown below, where C is fluid capacitance.

$$Q = C\frac{dP}{dt} \tag{10}$$

The pump was first modeled as a constant pressure source. Closer scrutiny revealed that when it was set to zero, the pump permitted no backflow through itself. This behavior is more analogous to a constant flow source or a current source, which behaves like an open circuit when set to zero.

The servo-valves turned out to be the elements which made the circuit highly non-linear. Although they dissipate energy, like the fluid resistances mentioned above, they don't satisfy the entrance length requirement for laminar flow, and thus produce turbulent flow. The constitutive law for these valves shows pressure drop to be proportional to the square of flow rate through the valve. The constant of proportionality includes the flow coefficient (Cv) which is a function of valve position, along with the specific gravity (SG) of the fluid.

$$Q^2 = Cv^2\,\frac{\Delta P}{SG} \tag{11}$$

A more exhaustive model could be pursued if the need arises – for instance, if certain elements in the circuit were replaced with more linear elements and a linear control algorithm were then implemented. With the circuit as it stands, the model can be used to predict the open loop response to a step input as being roughly similar to a first order linear response to the same input. The results to that test and those described in the following section will appear in Chapter 4.

3.3 Designing a Control Algorithm

Even if the system had been linear and linear control techniques had been applied, another problem would have arisen. In order to effectively assert feedback in a fluid power circuit, a controller should be able to specify either a constant pressure or a constant flow rate as its input to the circuit. In the case of the ram fluid power circuit, as it is currently designed, all the controller is able to specify is one resistance (R_3)in a flow divider which determines the input flow rate to the vessel (see Figure 5a). Figure 5b shows the equivalent flow source of the fluid power circuit. It was not necessary to include the switch, as the resistance can be made infinite by closing the valve, but it was included in Figure 5a to emphasize that very point.

A simplified analogous electrical scenario, in which the valve would simply be modeled as a mechanically-controlled on-off switch, is drawn schematically in Figure 5c. In this situation, the controller would control the position of the switch in order to achieve the desired voltage across the capacitor. The electrical analogy here is obviously simpler than the actual fluid power situation, for the valve not only has resistance, but it is also non-linear.

The types of tests to be run on the triaxial cell require ram fluid pressure is to be ramped up or down at a constant rate while keeping confining stress constant. The most straightforward way of doing this, considering the way the circuit is set up, is to divide the test into a number of incremental time steps, each with a corresponding pressure step. If, within the local environment of each time step, the final pressure is achieved by the final time, then globally, the actual pressure will closely follow the reference value. In fact, in the limit of an infinite number of time steps, the actual pressure would follow the reference value exactly.

The speed at which the valve may be operated will most likely be the limiting factor in determining the sampling rate. The valve's capabilities, in terms of speed, should be determined experimentally. Another thing to consider is how to meet the local final pressures, *LFP*'s, by the corresponding times. The average rate of pressure increase during each time step must be at least as great as the reference rate for the local endpoints to be attainable. *LFP*'s will most likely be reached before the end of their corresponding time step, in which case the valve could be closed for the remainder if the timestep. In order to stay close to the reference rate, *LFP* should not be overshot. Therefore, the valve should begin closing at a pressure below *LFP* in order to avoid overshoot. At what pressure it should begin closing requires knowledge of the rate of pressure increase. The rate of pressure increase in the vessel is directly proportional to the flow rate through the valve, which in turn is a function of valve opening and pressure drop across the valve (ΔP). Consequently, pressure rates should be tabulated as a function of ΔP and valve opening. Finally, a set of valve openings should be chosen which gives pressure increase rates close to but greater than typical reference rates. Also the time required to achieve chosen valve openings should be considered in relation to desired sampling periods, and the repeatability of valve positions should be verified.

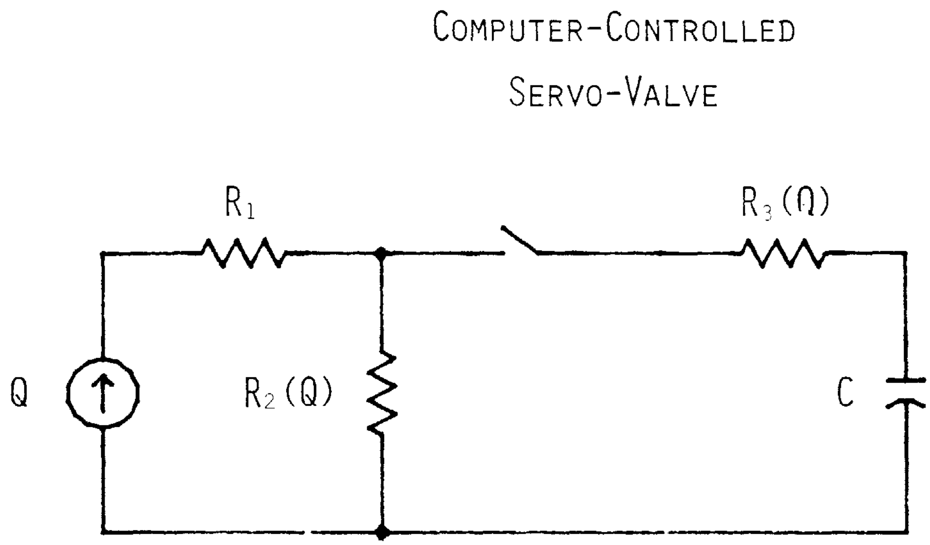

Figure 5a. Flow Divider of Fluid Power Circuit

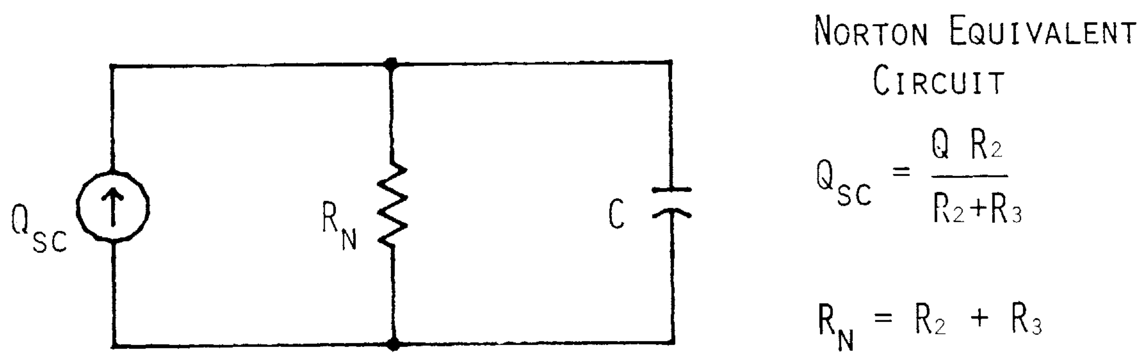

Figure 5b. Equivalent Flow Source

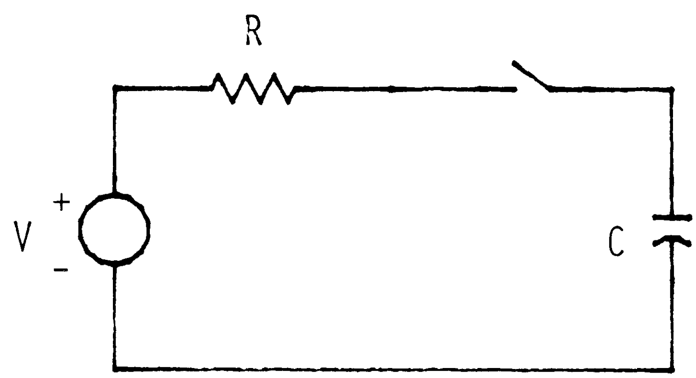

Figure 5c. Analogous Electrical Scenario with Mechanically-Controlled Switch

4. Test Results

4.1 Operating the Servo-valves

The effect of valve opening and pressure drop across the valve (ΔP) on flow through the valve and thus cell pressure were examined through a number of experiments. The results of those experiments, along with others having to do with timing characteristics and valve position repeatability, are reported in this chapter.

A brief explanation of the operation of the servo-valve used is in order because it is so critical in controlling cell pressure and because its characteristics will impose the most severe limitations on the control algorithm. First it will operate either manually or under computer control. It is a metering valve which may be positioned anywhere from fully open to fully closed. When under computer control, it receives control signals over three lines: *OPEN*, *CLOSE*, and *RESET*. Any *OPEN* or *CLOSE* command starts the valve moving in the appropriate direction until a *RESET* is issued or the valve reaches its preset endpoint. A valve will respond correctly to consecutive *OPEN* and *CLOSE* commands, without the issuance of a *RESET*, provided the commands are not given less than 400 ms apart. There is a delay of about 50 ms from the time a command is issued until the valve begins to move.

It happens to be the case not only that the valve turns at a constant rate, but also that the valve flow coefficient (Cv) is approximately linear in the region the valve was used. This means that the Cv for the valve is linearly proportional to length of time the control signal was asserted. The plots in this chapter have the valve position axis scaled in units of Cv.

4.2 The Effects of Valve Position and Δ P on Vessel Pressure

The first tests done on the ram fluid power system were open loop tests in which a step input in pressure was applied to the vessel and its pressure response was monitored. The vessel was completely filled with fluid as the ram piston has yet to be installed. With the drain valve closed and the control valve completely open, the vessel was slowly brought up to somewhere near 5000 psi. All tests were conducted above 5000 psi so that any air in the system would be completely compressed and wouldn't add to the system's compliance. After the vessel had equilibrated with the pump somewhere between 5000 and 6000 psi, the valve was closed, isolating the vessel from the pump. The pump was then taken up to pressures anywhere from 3000 to 10,000 psi above that in the vessel. Finally, the valve would be opened and the pressure in the vessel would rise accordingly.

The results of these tests for a valve opening time of 500 ms (equivalent to a Cv of about 0.0155) are presented below. Data was taken with the COLECT program on the Minc-11, at a sampling periods ranging from 0.05 to 25 seconds. Plots of the data from these runs were made on the Houston Instruments plotter using the NEWPLT program in order to get an idea of the shape of the curves. The data was analyzed by STATS, a curve fitting program on the Vax 11-750.

Results, which can be found in Table 2, indicate that, at least to one exponential time constant, the system response somewhat resembled that of a linear, first order system. Figure 6 shows a typical plot.

The next set of tests also examined the response of vessel pressure, but on a much smaller time scale. The test itself was set up in much the same way as the one previously described, but was conducted differently. At predetermined pressures, the control valve was opened to one of three settings tested and vessel pressure was sampled every 0.05 seconds, for about 10 seconds. The pressure was then allowed to reach the next test pressure, where the valve was then closed and the next test would follow.

The purpose of this test was to observe pressure response on the same time scale as a sampling period of the control program. Data was taken, plotted, and analyzed using the same programs as above and some interesting results were found. Out to at least to 8 seconds after the valve opened, the rate of pressure increase was very constant. This can be seen in Table 3 by noting the values of the correlation coefficient, R^2, for the straight line fits. Every value but one is greater than 0.9900. It can also be seen in the plots which were made for the largest and smallest valve setting for the largest and smallest pressure differentials tested. These plots can be found in Figure 7.

One final test to examine the effect of valve position on vessel pressure was conducted. In this test, the valve was opened, and then very quickly closed to see if the pressure would respond as expected. Three different valve settings were pulsed open for 6 seconds each. All had a pressure differential between 7000 and 7500 psi across them. The rate of pressure increase remained quite linear while the valves were open, and fell off to zero as soon as the valves were closed, as expected. Results appear in Figure 8a. In another part of the test, one valve setting was pulsed open for only three seconds. This was run at three different pressure differentials. Although the pressure signal on those plots seems rather noisy, part of the reason is that the scale is much larger than the other plots. Nonetheless, these plots show the same pressure response as the 6 second pulses did and can be seen in Figure 8b.

A listing of valve control programs appears in Appendix B.

4.3 Other Tests

Valve setting and a pulse length can combine to give desired flow characteristics and thus desired vessel pressure response. However, the ability to repeatably position a servo-valve should not be assumed. Experimentation revealed that the valves could be positioned repeatably only for opening times of 400 ms or more. In the course of testing, the valve's position, for opening times of 400 ms or more, was observed to be repeatable to within .1%, which is quite reliable. One possible explanation of why shorter opening times weren't reliable might be that the delay of the valve (approximately 50 ms) became significant at times less than 400 ms. This limitation explains why valve openings which would have given pressure rates closer to those desired, were not tested. This discussed further in Chapter 5.

Also, the time it takes the valve to reach a desired positioned is not negligible. As seen Figure 9, the time the valve is in motion, or the transition time, (a total of 1 second in that case) can occupy a significant portion of the time of the pulse, or the excursion time. In this case, transition time accounts for approximately 28.5% of the excursion time. This effect is also discussed in Chapter 5.

	Initial Pressure (P_I)	Final Pressure (P_F)	Total Pressure (P_F-P_I)	Correlation Coefficient (R^2)
1	5,432	8,919	3,486	0.9754
2	5,366	10,367	5,001	0.9701
3	5,714	10,957	5,243	0.9786
4	5,875	12,848	6,973	0.9792
5	5,530	13,282	7,752	0.9800
6	5,567	14,199	8,631	0.8908
7	5,665	15,041	9,376	0.9827

Table 2. Exponential Curve Fits To Open Loop Pressure Data

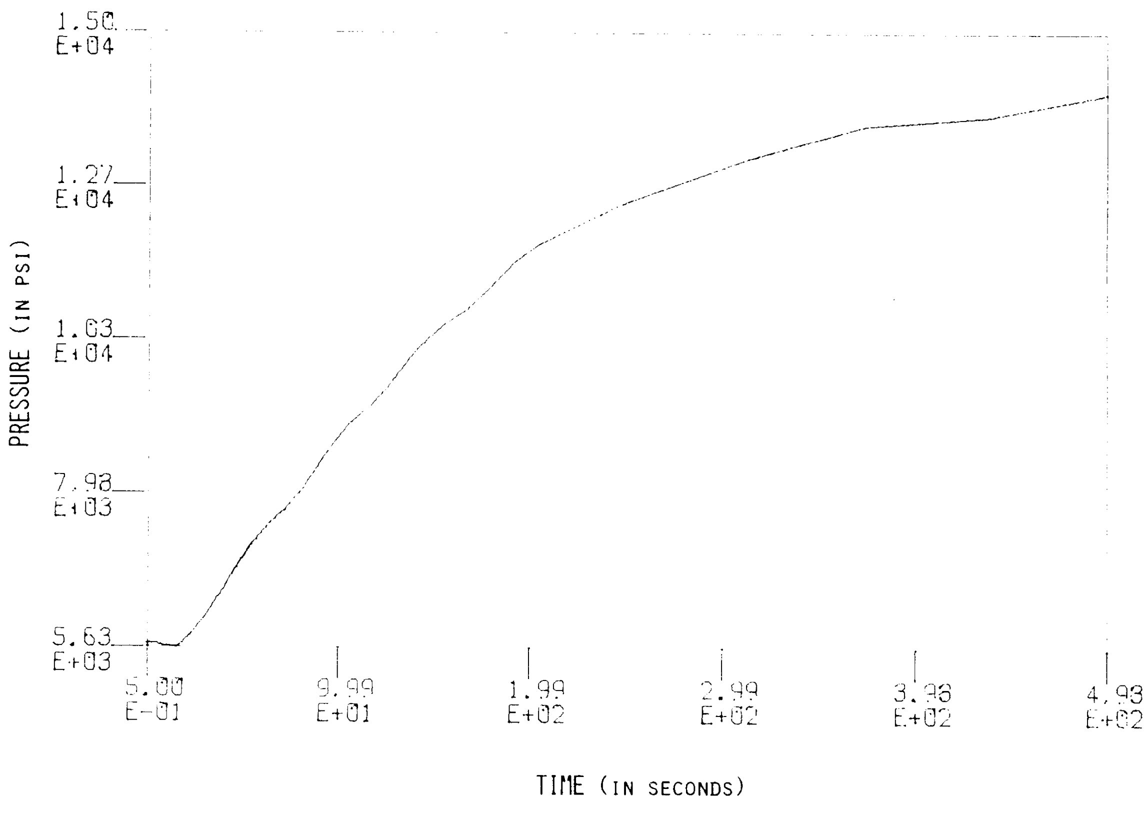

Figure 6. Open Loop Response of Pressure to a Step Input

	Pressure Drop (ΔP)	Valve Opening Time	Pressure Increase Rate	Correlation Coefficient (R^2)
1	10,048 psi	400 ms	37.91 $\frac{psi}{s}$	0.9980
2	8,950	400	34.64	0.9980
3	7,884	400	28.61	0.9972
4	7,016	400	23.28	0.9893
5	5,901	400	26.70	0.9935
6	9,718	500	42.32	0.9953
7	8,620	500	38.98	0.9917
8	7,852	500	44.72	0.9951
9	6,798	500	37.33	0.9961
10	5596	500	40.20	0.9962

Table 3. Pressure Rates for Various ΔP's and Valve Opening Times

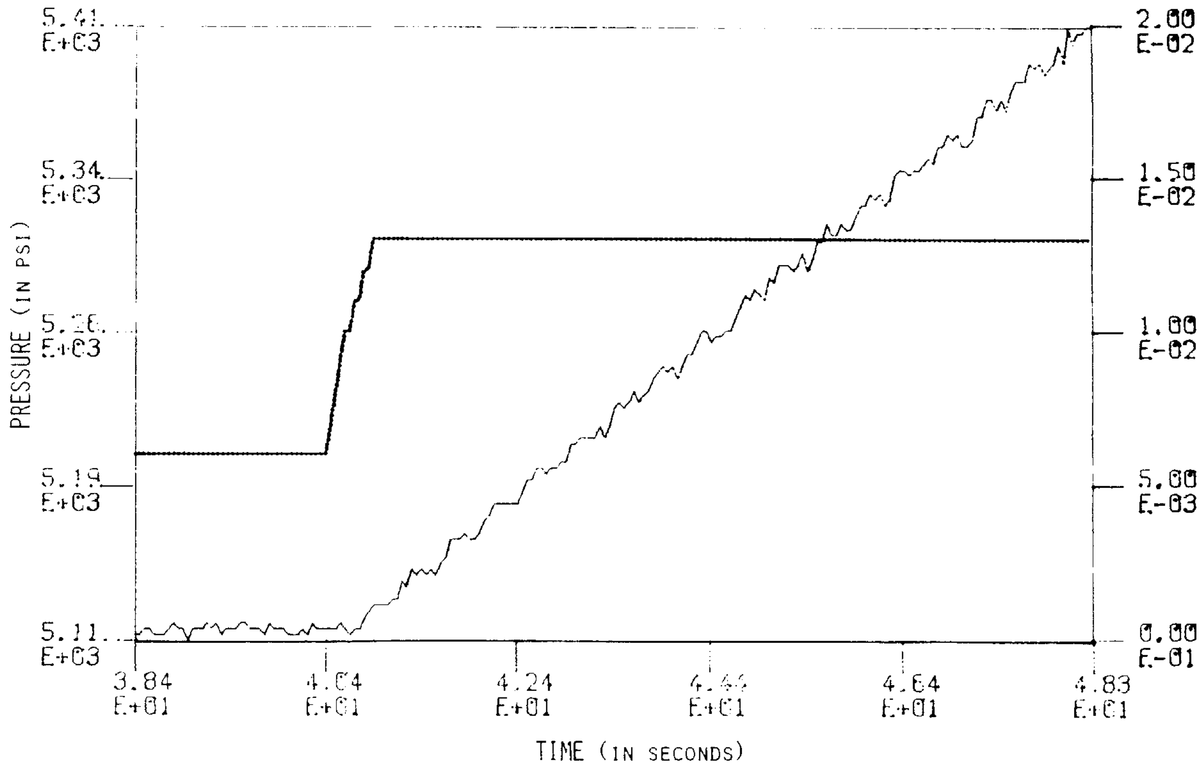

Figure 7a. Pressure Rates for Min ΔP for Valve Opening Time of 400 ms

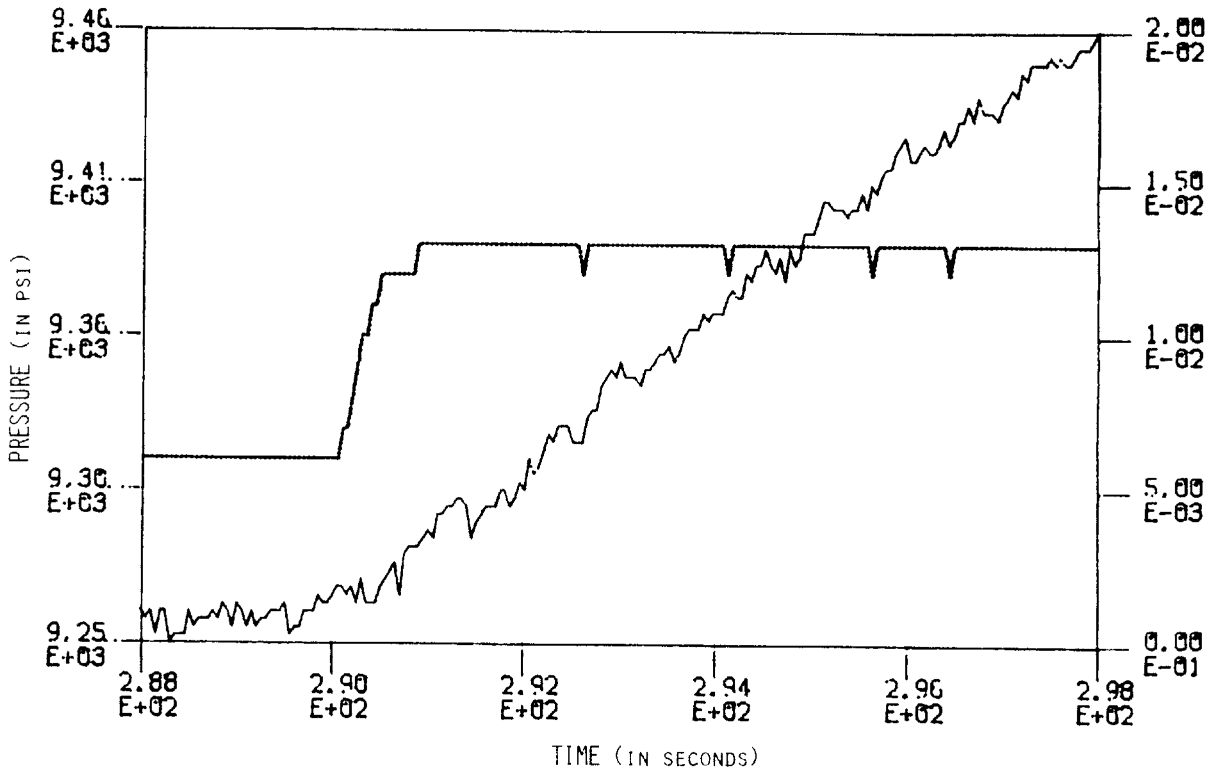

Figure 7b. Pressure Rates for Max ΔP for Valve Opening Time of 400 ms

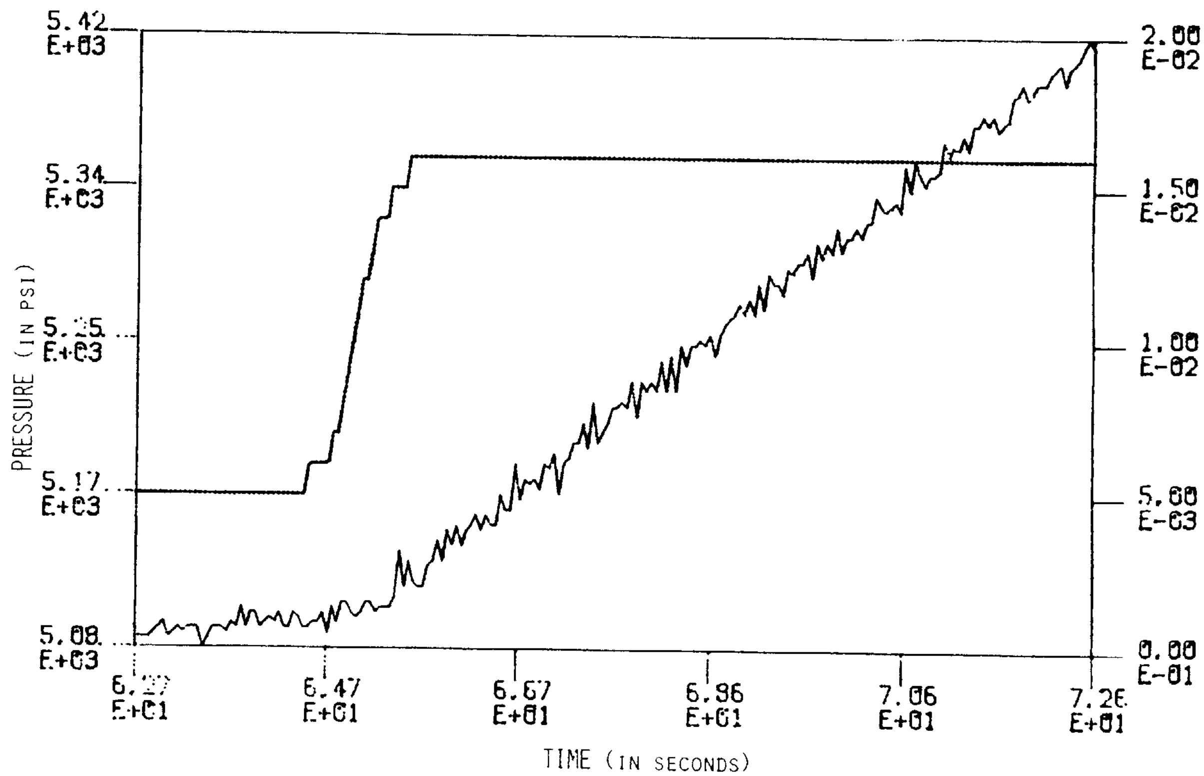

Figure 7c. Pressure Rates for Min ΔP for Valve Opening Time of 500 ms

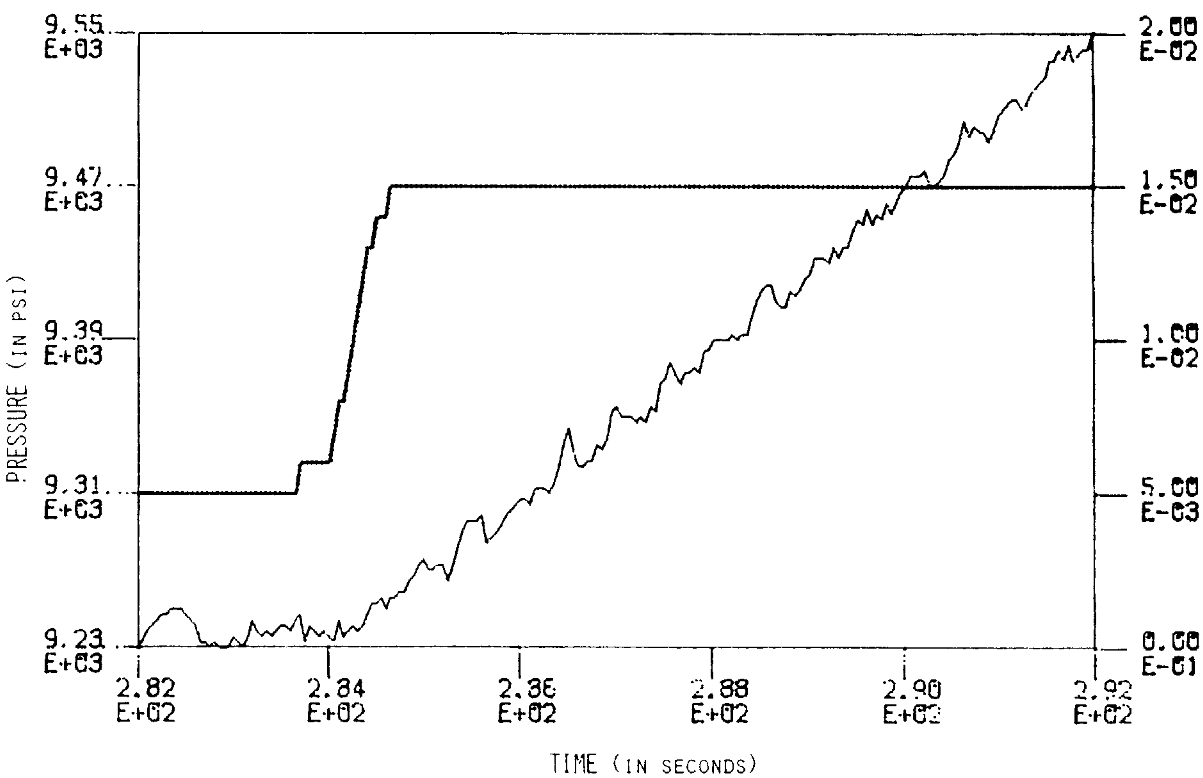

Figure 7d. Pressure Rates for Max ΔP for Valve Opening Time of 500 ms

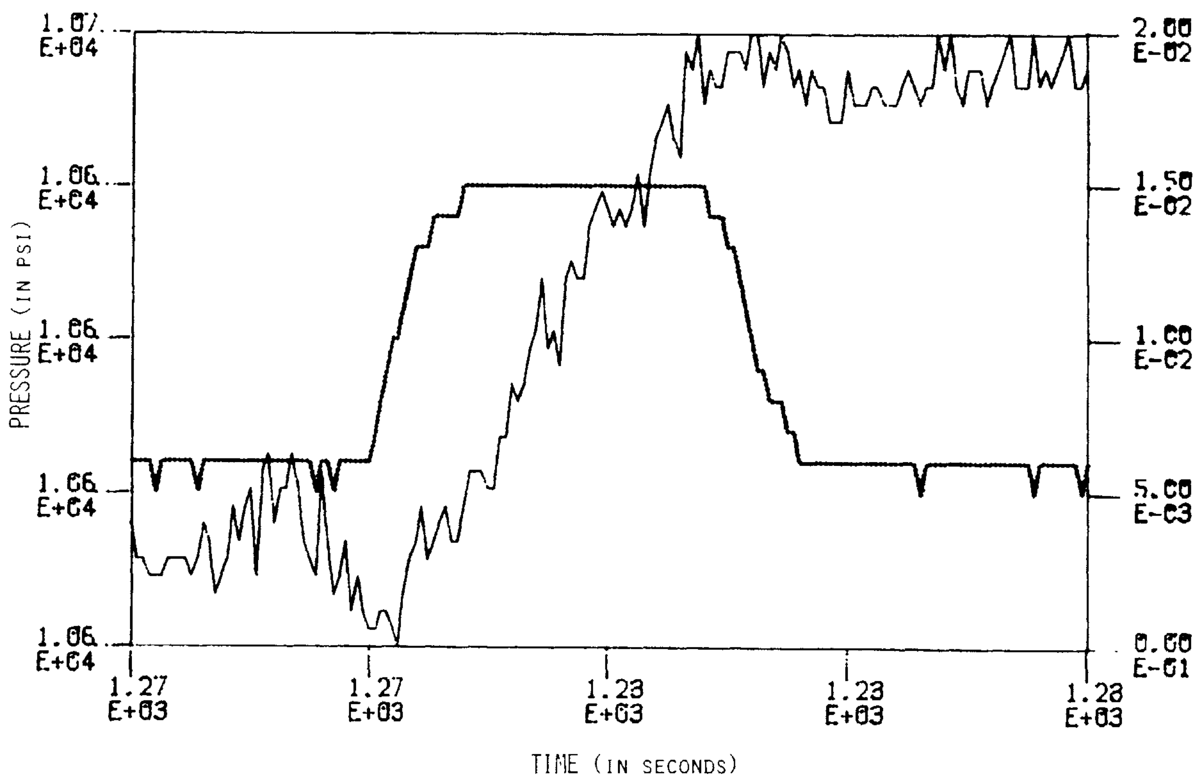

Figure 8a. Pressure Response: Valve Opening Time of 500 ms, Pulse Width of 3 Seconds

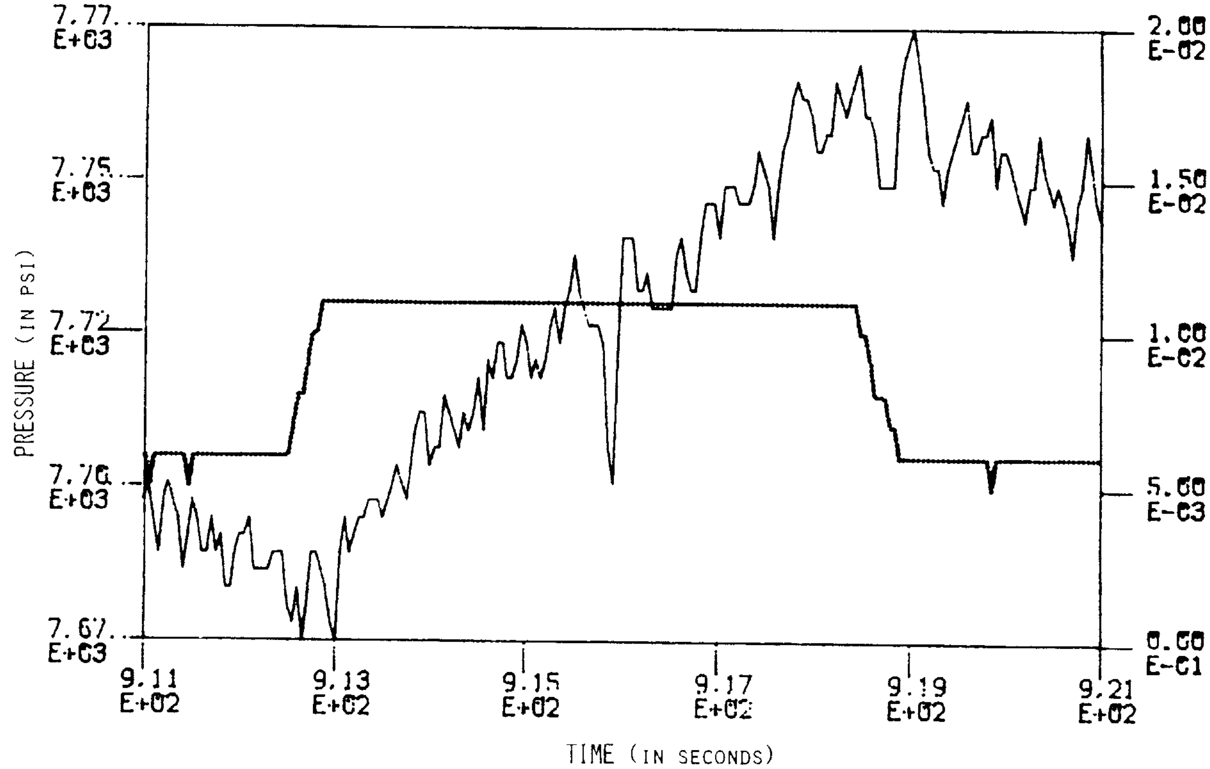

Figure 8b. Pressure Response: Valve Opening Time of 500 ms, Pulse Width of 6 Seconds

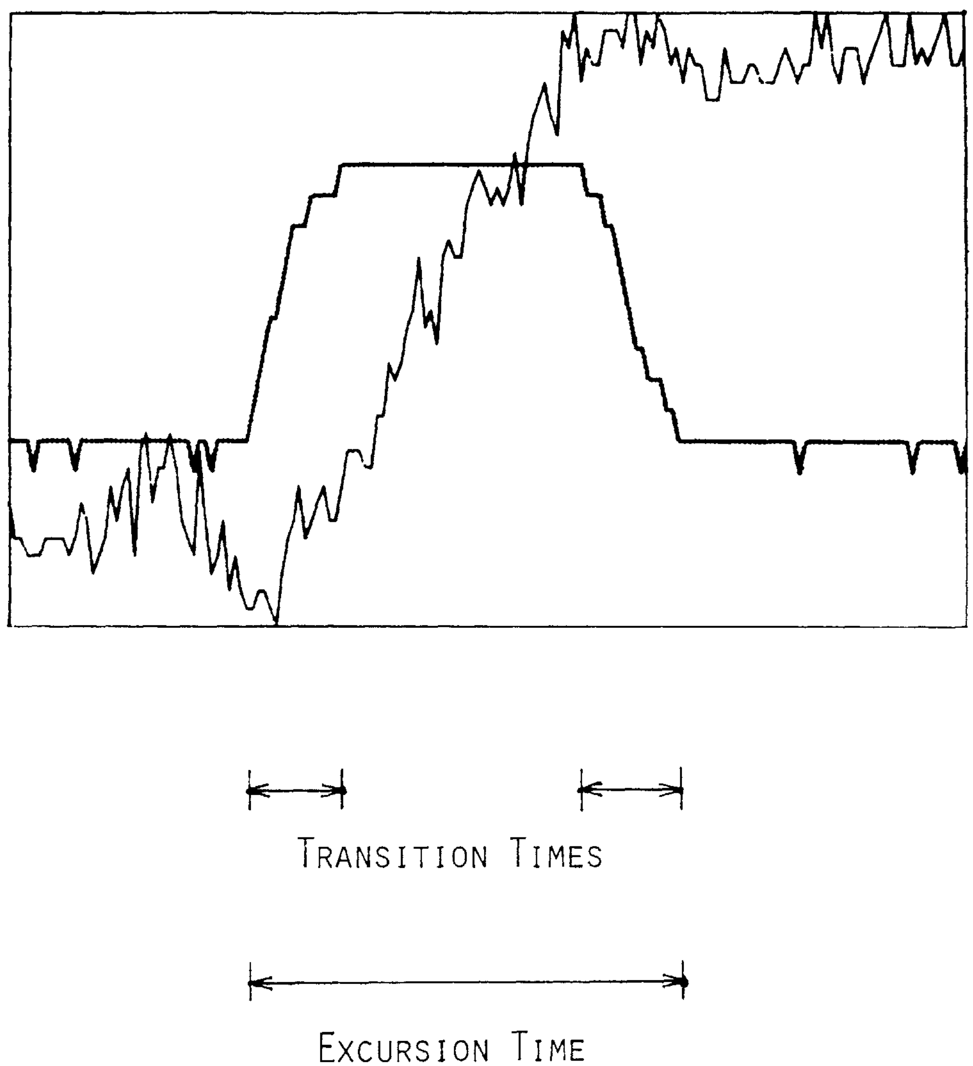

Figure 9 Transition Time Compared With Excursion Time

5. Discussion of Results

The control algorithm described in Section 3.3 and developed in full detail below has yet to be implemented in a program. However, since it soon will be on the IBM PC, consider it implemented in a hypothetical program for the purpose of the following discussion. It was found in Chapter 4 that pressure rises at a nearly constant rate for at least 8 seconds after the valve opens. This rate varies depending on valve opening and, for each valve opening, on ΔP. There was no apparent correlation between rate and Δ P, even for tests conducted at the same valve opening. I can only speculate as to an interpretation of these results, although it is undoubtedly due to a combination of several individual effects. However, it is quite useful in predicting vessel pressure vs. time, which is done by the control algorithm.

In order for any type of control program to operate, it must have a reference function with which it generates reference values as a function of time. The action of the controller at each time step depends on the difference between the generated reference value and the measured actual value for that time step. The time step, or *sampling period*, is usually made as small as is necessary to prevent large excursions from the reference function. If the system output being measured tends to change at a fast rate, a smaller sampling period is usually required.

Consider a typical run, where the experimenter would input the starting pressure and the desired rate of pressure increase, or *reference rate*. He would also input the sampling period. The reference function for this control program would be the equation of a line relating pressure to time. Its slope is equal to the reference rate and its y-intercept is equal to the starting pressure, with time initialized to zero. Before the run begins, an array of reference pressures corresponding to sampling times is generated. Also stored are experimentally determined values of pressure rates, referenced according to both valve opening and ΔP. Then, the valve opening having pressure rates closest to, yet greater than, the reference rate for all values of ΔP is chosen. The reference pressure corresponding to the end of the first sampling period and the pressure rate corresponding to the current ΔP are both read from their respective arrays. Following is a detailed explanation of the control algorithm used within the pressure sampling loop.

Let the "global" reference ramp be divided into a number of "local" ramps, each one corresponding to the pressure rise during one sampling period and each one terminating at a local final pressure *LFP*. Assuming the valve is initially closed, it begins opening at time = 0. While the *actual pressure* is rising, the pressure at which the valve will be instructed to close is being computed and will be referred to as the *closing pressure*. If the valve is not instructed to close until the actual pressure equals the *LFP*, it will overshoot the *LFP* due to the additional pressure increase during valve transition time. Since both valve transition time and pressure rate are known an *offset pressure* may be computed which equals the amount of pressure increase that would occur while the valve closed *if the pressure rate remained constant.* Since the pressure rate decreases to zero as the valve closes, the offset pressure represents an upper bound. The closing pressure may now be computed by the following equation.

$$\textit{closing pressure} = LFP - \textit{offset pressure}$$

When the actual pressure reaches the closing pressure, the valve is instructed to close. This most likely happens well before the end of the sampling period since pressure rates will generally be much greater than reference rates. An explanation of why this is so appears in Section 4.3. If the computed value of the offset pressure was used, the actual pressure should undershoot the *LFP* by an amount equal to the negative *error pressure*. An overshoot would create a positive error pressure. A "local" ramp and its associated pressures are shown in Figure 10.

It should be noted that the error pressure is not cumulative–i.e. it is independent of the error for the previous time step and has no reason to grow as the run progresses. This is an indication of the algorithm's *stability*. The error pressure can be made less negative, or even positive by multiplying the offset pressure by a constant between 0 and 1. In the extremes, a value of 0 will lead to the maximum possible overshoot, while a value of 1 will lead to the maximum possible undershoot. This constant could be left as an input parameter, specified by the experienced user or left to equal a default value.

This algorithm can be implemented, as described, using the IBM PC and the Keithley DAS Data Acquisition System to communicate with the pressure transducers and the servo-valves. A discussion of improvements and a plan for implementation can be found in Chapter 6.

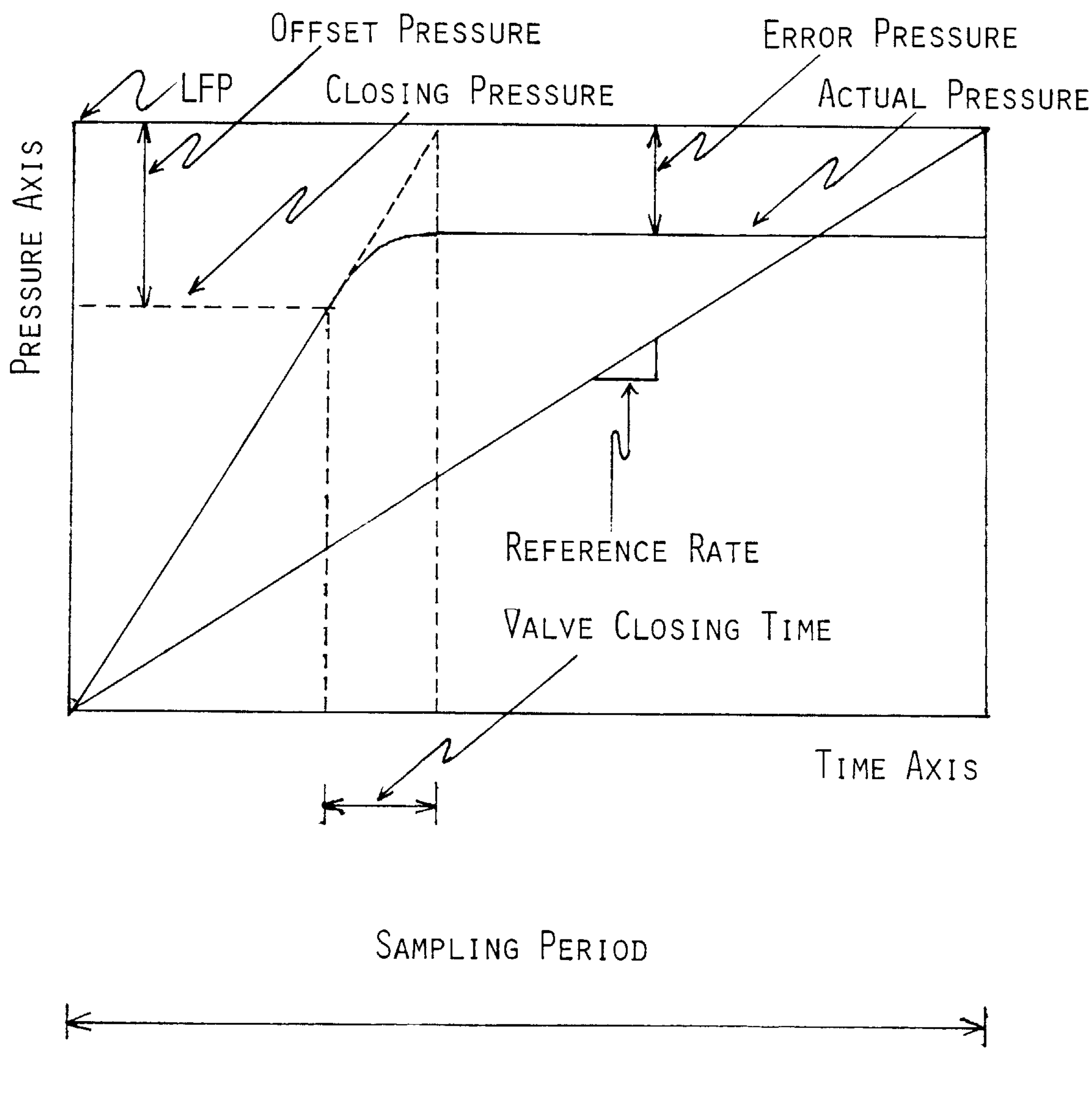

Figure 10 "Local" Reference Ramp and its Associated Pressures

6. Conclusions and Recommendations

The problem of controlling hydraulic fluid pressure in a pressure vessel by regulating flow through a servo-valve turned out to be about as interesting as it was difficult. Quite a few "intuitive solutions" which came up in the early stages of the project and were put on the "back burner" resurfaced towards the end when rigorous analysis had failed.

If the circuit were to be redesigned, more of the pressure control should be asserted via the pump, and valves should be used more as switches, and less as variable resistances. Also, even if the circuit is left in its present form, a remote controlled servo-valve should be placed in the circuit between the control valve and the vessel. This would allow for a more steady flow situation in the circuit as pressure was being ramped up. Also, it would allow for pressure to be bled off during ramping if a local final pressure, *LFP* is overshot, thus giving the controller the ability to raise or lower pressure at any time. A pressure transducer should be placed in the circuit which reads pump output pressure. This would be useful in testing valve characteristics, and would allow the pump to be set more accurately.

Unfortunately, this algorithm has not actually been tested and proven. I am confident the pressure in the triaxial cell can be controlled in its present configuration, using the previously mentioned hardware and software and I feel that a usable triaxial test system would result. I would encourage improvements to this algorithm be made after it is operational when their value may be assessed immediately. I have one new version in mind already in which the pressure is allowed to fall below the reference half the time and rise above the reference half the time, as opposed to always being above it. Roughly speaking, it would start off with the valve open, exactly the same as before. The valve would be closed at the appropriate time. However, when the next sampling period began, instead of opening again, it would stay closed, allowing the actual pressure to drop below the reference value. The valve would then be opened in just enough time for the actual pressure to reach the following *LFP*. The valve would remain open as pressure passes through the *LFP* at which point the algorithm would have completed one cycle.

Many other versions are possible and only experience will show which are most effective.

References

1. Bishop, A. W. and D. J. Henkel, "The Measurement of Soil Properties in the Triaxial Test", Edward Arnold (Publishers) Ltd., London, 1957.

2. Hawkes, I. and M. Mellor, "Uniaxial Testing in Rock Mechanics Laboratories", Engineering Geology, vol. 4, no. 3, Elsevier Publishing Company, Amsterdam, 1970.

3. Martin, R. T., C. Lee, J. Egan, R. Fleischner, A. Woo, and M. P. Cleary, "Material Properties for Cement Paste and for Cement Mortar", Report REL-84-7, Dept. of Mechanical Engineering, MIT, 1984.

4. Shearer, J. L., A. T. Murphy, and H. H. Richardson, "Introduction to System Dynamics", Addison-Wesley Publishing Company, Reading, MA, 1971.

5. Vogeler, S. and M. P. Cleary, "Strength Variations of Laboratory Cast Cement as a Function of Molding Water Content and Curing Time", Report REL-84-13, Dept. of Mechanical Engineering, MIT, 1984.

6. White, F. M., "Fluid Mechanics", McGraw-Hill Book Co., New York, 1979.

7. Wright, T. B., N. P. O'Driscoll, J. Ashley, A. Sparks, J. Sununu, and M. P. Cleary, "Laboratory Simulations of Hydraulic Fracture Interaction", Report REL-84-8, Dept. of Mechanical Engineering, MIT, 1984.

Appendix A

The pressure vessel in the triaxial system is an HIP R7-24-30, 30,000 psi (2068 MPa)vessel manufactured by High Pressure Equipment Company, Inc. of Erie, Pennsylvania.

The pump is made by SC Hydraulics Co.

The computer control circuitry driving the servo-valves is made by Advanced Pressure Products of Ithca, New York. The valves, themselves, are also made by HIP. The control valve is model number 60-13HF6 and the drain valve is a 60-14HF4.

The data acquisition system is made by Keithley DAS and contains a 14-bit A/D converter and digital output capabilities. It comes with its own software which amount to nothing more than basic callable subroutines.

The computer in the system is an IBM PC with 512 kilobytes of memory.

Appendix B

```
     LOAD"ramp.bas
Ok
LIST
500 CALL INIT
510 CALL INTON
520 CALL IONAME'("DO.B",5,"B")
530 CALL IONAME'("OPEN",5,11)
540 CALL IONAME'("CLOSE",5,12)
550 CALL IONAME'("RESET",5,13)
560 CALL IONAME'("AI.0",1,0,14)
570 CLS
580 PRINT
590 PRINT
600 CALL DIGWRITE'("DO.B",56.0)
650 INPUT "SELECT POSITION 1, 2, OR 3."; NUM
660 IF NUM=1 THEN TIM#=40 ELSE IF NUM=2 THEN TIM#=45 ELSE TIM#=50
670 VOT=TIM#*10
671 PRINT
672 PRINT
673 INPUT "SELECT PULSEWIDTH 3, 4, 5, OR 6."; WID
674 PW#=WID*100
680 PRINT
690 PRINT
700 PRINT "VALVE OPENING TIME = ";VOT;" MILLISECONDS. "
702 PRINT
704 PRINT
705 PWID=PW#*10
706 PRINT "PULSE WIDTH = ";PWID;" MILLISECONDS. "
710 PRINT
712 PRINT
770 T0#=0:T1#=0
780 INPUT "HIT <CR> WHEN READY TO OPEN VALVE."; DUMMY$
790 CALL TIMERSTART'(0,1)
800 CALL DIGWRITE'("OPEN",0.0)
830 CALL TIMERREAD'(0,T0#)
840 IF T0# < TIM# GOTO 830
845 CALL DIGWRITE'("OPEN",1.0)
850 CALL DIGWRITE'("RESET",0.0)
852 CALL TIMERREAD'(1,T1#)
854 IF T1# < PW# GOTO 852
855 CALL DIGWRITE'("RESET",1.0)
856 CALL DIGWRITE'("CLOSE",0.0)
860 GOTO 570
870 END
Ok
```

```
 LOAD"cvtest.bas
Ok
LIST
100 CALL INIT
105 CALL INTON
110 CALL IONAME'("DO.B",5,"B")
120 CALL IONAME'("OPEN",5,11)
130 CALL IONAME'("CLOSE",5,12)
140 CALL IONAME'("RESET",5,13)
142 CALL IONAME'("AI.0",1,0,14)
145 CLS
146 PRINT
147 PRINT
148 CALL DIGWRITE'("DO.B",56.0)
149 INPUT "HIT <CR> TO CLOSE VALVE."; DUMMY$
150 CALL DIGWRITE'("CLOSE",0.0)
151 PRINT
160 PRINT
170 INPUT "SELECT POSITION 1, 2, OR 3."; NUM
180 IF NUM=1 THEN TIM#=40 ELSE IF NUM=2 THEN TIM#=45 ELSE TIM#=50
190 VOT=TIM#*10
200 PRINT
205 PRINT
210 PRINT "VALVE OPENING TIME = ";VOT;" MILLISECONDS. "
220 CALL DIGWRITE'("DO.B",56.0)
225 PRINT
227 PRINT
230 PRINT "CONTROL SIGNALS INITIALIZED."
240 PRINT
250 PRINT
260 T0#=0:T1#=0
270 INPUT "HIT <CR> WHEN READY TO OPEN VALVE."; DUMMY$
280 CALL DIGWRITE'("OPEN",0.0)
290 CALL TIMERREAD'(0,T0#)
300 T1# = T0# + TIM#
310 CALL DIGWRITE'("OPEN",1.0)
320 CALL TIMERREAD'(0,T0#)
330 IF T0# < T1# GOTO 320
340 CALL DIGWRITE'("RESET",0.0)
350 GOTO 145
360 END
Ok
```